

A Multifunctional Chiral Metasurface with Asymmetric Transmission and Linear-Polarization Conversion

AFZAL Ahmed, CAO Qunsheng*, MUHAMMAD Sajjad

College of Electronics and Information Engineering, Nanjing University of Aeronautics and Astronautics,
Nanjing 211106, P. R. China

(Received 20 May 2024; revised 20 August 2024; accepted 25 August 2024)

Abstract: In this paper, a multifunctional chiral metasurface is presented to achieve asymmetric transmission (AT) and linear-polarization conversion (LPC). The designed metasurface consists of a cross swords-like shape and two holes in the lower side of the unit cell. In the frequency band from 8.3 GHz to 10.4 GHz, AT is realized with more than 90% efficiency and the same chiral metasurface transforms linear polarized wave into its orthogonal counterpart with high efficiency. For LPC, the polarization conversion ratio (PCR) is greater than 95%. The proposed metasurface is stable against the incident angles of striking electromagnetic (EM) waves up to 60° for both operations of AT and LPC.

Key words: chiral metasurface; polarization conversion; asymmetric transmission; plasmon resonances

CLC number: T8 **Document code:** A **Article ID:** 1005-1120(2024)S-0021-06

0 Introduction

Metamaterials, a novel class of electromagnetic materials, have garnered significant interest due to their remarkable capacity for manipulating electromagnetic waves and their compact spatial demands. The investigation of metamaterials facilitates the realization of several distinctive phenomena, such as polarization conversion. Control of polarization is an important characteristic of electromagnetic waves used in many applications including imaging^[1] and meta-lens antennas^[2], although there are limitations of low efficiency and incident angles which affect the performance of mostly polarization converters. To overcome such issues of low efficiency^[3] and incident angles^[4], an alternative way uses chiral metamaterials which is a special group of metamaterials for controlling the polarization. Chiral metamaterials are characterized by the lack of mirror symmetry, meaning that their chiral configuration cannot be superimposed over its mirror reflection. The asymmet-

ric nature of chiral metasurface makes it important for asymmetric transmission^[5-6] and linear or circular polarization conversions^[7-8].

Refs. [9-10] proposed the use of a single-layered reflective surface to achieve cross-polarization conversion (CPC) with consistent performance under different incident angles. Additionally, a metamaterial in the shape of a twisted Hilbert^[11] curve was suggested as a means to accomplish the conversion of linear polarization to circular polarization. The metasurface described in Ref. [12] successfully accomplished both the functions of CPC and conversion of linear polarization to circular polarization. Chiral metasurfaces were utilized to investigate a phenomenon called asymmetric transmission (AT), where the total transmission of electromagnetic waves changes depending on the direction of propagation across the metasurface^[13]. Achieving a 60% efficiency in the frequency region of 5.5—5.9 GHz was demonstrated in Ref. [14] through the use of 2D-chiral split rings. A dual-layered arrange-

*Corresponding author, E-mail address: qunsheng@nuaa.edu.cn.

How to cite this article: AFZAL Ahmed, CAO Qunsheng, MUHAMMAD Sajjad. A multifunctional chiral metasurface with asymmetric transmission and linear-polarization conversion[J]. Transactions of Nanjing University of Aeronautics and Astronautics, 2024, 41(S): 21-26.

<http://dx.doi.org/10.16356/j.1005-1120.2024.S.003>

ment of inclined metal strips was suggested to accomplish a wide frequency range (8.58—9.73 GHz) for antenna transmission, with a transmission magnitude of 0.9^[15]. In addition, a study was conducted to investigate the stable response of an incidence angle up to 60° in order to achieve an AT with a transmission coefficient of 0.95^[16]. A recently developed chiral structure has achieved an efficiency of about 80% over the frequency range of 18.6—20.8 GHz^[17].

In this paper, a bi-layered multifunctional chiral metasurface is proposed which performs AT and linear-polarization conversion (LPC). The designed structure of a unit cell is composed of cross swords-like shape with two holes in the lower portion. The operations of AT and LPC are achieved with more than 80% AT parameter in the frequency range of 8.3—10.4 GHz and 85% polarization conversion ratio (PCR), respectively. The proposed chiral structure is angularly stable against the varying angles of incident electromagnetic (EM) waves for AT as well as LPC operation up to 60°.

1 Metasurface Unit Cell Design

The chiral metasurface under consideration comprises a cross swords-like shape with two holes positioned on both sides of a substrate that is sandwiched between them, as depicted in Figs.1(a—c). Fig.1(c) illustrates that the cross swords-like shape pattern on the lower layer is a 90° rotated replica of the cross swords-like shape on the upper layer. The absence of mirror symmetry can be attributed to the 90° rotation of the lower structure. Therefore, the detection of AT is facilitated by the utilization of the engineered metasurface, which exhibits mirror asymmetry.

The metallic cross swords-like shapes at the top and bottom are composed of copper with a thickness of 35 μm and a conductivity of 5.8×10^7 S/m, respectively. The dimensions of the unit cell of the top and bottom copper layer, as seen in Fig.1(b), have been optimized. These parameters are as follows: $P = 7$ mm, $a = 1$ mm, $b = 0.4$ mm, $l = 4.7$ mm, $d = 0.4$ mm, $c = 1.3$ mm, and $r =$

0.5 mm. The substrate Rogers RT5870 has a thickness of 0.7 mm, a relative dielectric constant of 2.3, and a loss tangent of 0.001 2.

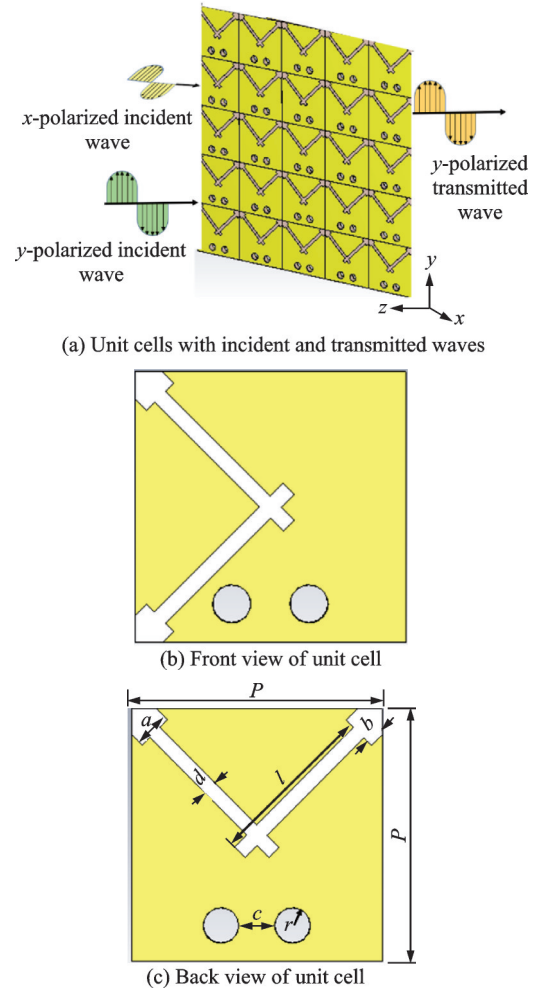


Fig.1 Schematic of the proposed chiral metasurface

2 Simulation Results and Analysis

2.1 Asymmetric transmission

The simulated results of transmission coefficients are obtained by using the CST Microwave Studio software. In the xy plane, the periodic boundary conditions are applied, while in the z direction, the linear polarized wave is incident on the metasurface in forward and in backward directions. The simulated curves of transmission coefficients in the case of forward and backward direction propagation are depicted in Fig.2 and Fig.3. As can be seen in Fig.2 that in the case of forward direction propagation, the values of cross-polarized coefficients T_{yx}^f and T_{xy}^f are noted as 0.95 and 0.05 in the frequency

band of 8.3–10.4 GHz, while for backward direction propagation the values of T_{yx}^b and T_{xy}^b are totally different from forward transmission coefficients for the same frequency band, as shown in Fig.3. It is realized that in forward direction propagation, the designed structure transforms x -polarized wave into y -polarized wave during transmission, while in backward transmission, the y -polarized wave changes to x -polarized wave. The value of T_{yx}^f is equal to T_{xy}^b which proves the phenomena of asymmetric transmission.

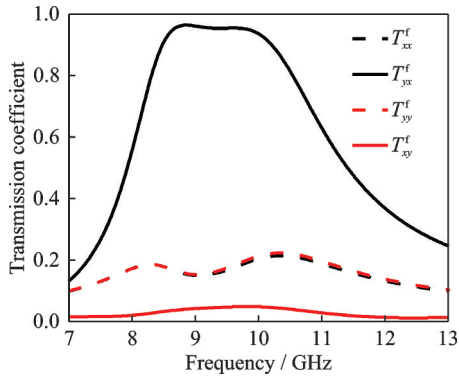


Fig.2 Transmission coefficients of linear x -polarized and y -polarized EM waves in forward direction

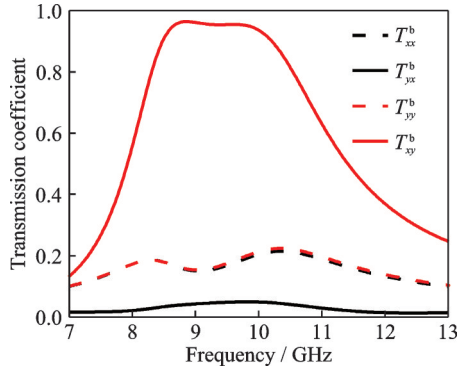


Fig.3 Transmission coefficients of linear x -polarized and y -polarized EM waves in backward direction

To calculate the asymmetric transmission parameter for both x - and y -polarized incident EM waves, the following equation can be used

$$\Delta_{\text{lin}}^x = |t_x^f|^2 - |t_x^b|^2 = |t_{xx}^f|^2 + |t_{yx}^f|^2 - |t_{xx}^b|^2 - |t_{yx}^b|^2 = |t_{yx}^f|^2 - |t_{xy}^f|^2 = -\Delta_{\text{lin}}^y \quad (1)$$

where the superscripts ‘f’ and ‘b’ are used to express the forward and backward EM wave propagations.

In Fig.4, the AT parameter for x -polarized in-

cident EM wave is plotted. The value of AT parameter is calculated by using Eq.(1) and it can be examined that the value of AT parameter Δ_{lin}^x is greater than 0.9 for the whole band from 8.3 GHz to 10.4 GHz.

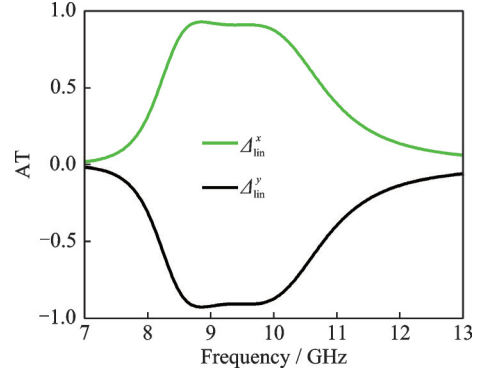


Fig.4 AT parameter at normal incidence

2.2 Linear-polarization conversion

Another important parameter is PCR which is used for measuring the LPC efficiency and can be defined as

$$\text{PCR} = |t_{yx}|^2 / (|t_{yx}|^2 + |t_{xx}|^2) \quad (2)$$

where $|t_{yx}|$ and $|t_{xx}|$ denotes the cross polarized and co-polarized transmission coefficient magnitudes, respectively.

Simulated PCR at normal incidence is shown in Fig.5. From Fig.5 it can be seen that the value of PCR is more than 0.9 which means that the proposed chiral metasurface performs operation of polarization conversion efficiently.

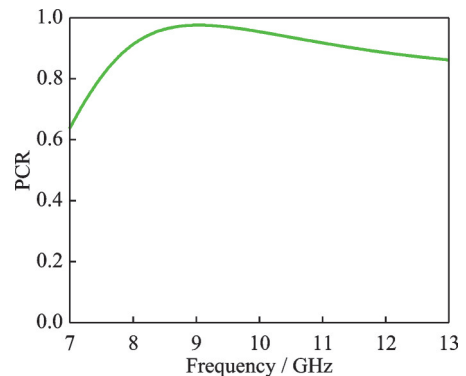


Fig.5 Simulated PCR at normal incidence

2.3 Angular stability

For the use of metasurfaces in real time scenarios, the behavior of metasurface should be stable

against the varying incident angles of striking EM waves. In this paper, the designed chiral metasurface shows stability up to 60° in case of both operations of AT and LPC. The angular stability results for both operations are illustrated in Fig.6 and Fig.7.

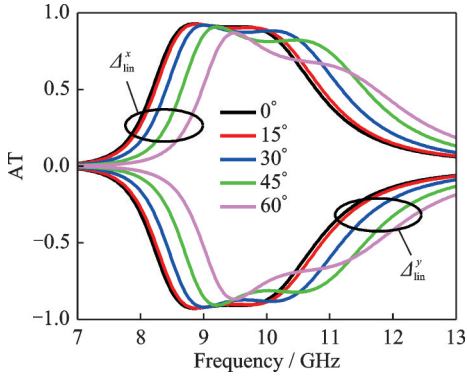


Fig.6 AT parameter under varying incident angles

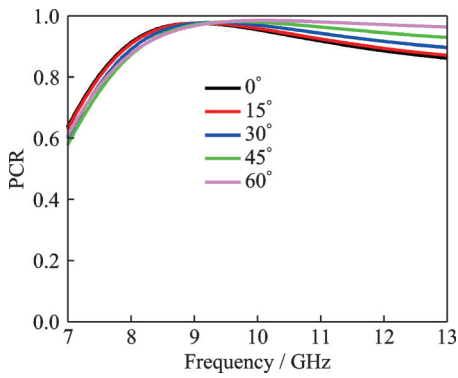


Fig.7 PCR under varying incident angles

2.4 Surface current distribution

The distribution of surface current on metallic layers located at the top and bottom of the proposed structure can be employed to comprehend the physical principle that explains the AT phenomena and the conversion of linear cross-polarization. The surface current distributions for forward transmission orientation are illustrated in Fig.8 at a resonance frequency of 10 GHz. Fig.8 illustrates that the top metal layer acts as an electromagnetic vibrator at 10 GHz, causing the bottom metallic layer to become stimulating due to the forward illumination. In the forward direction of propagation, only x -polarized incident waves induce current distributions, as illustrated in Fig.8. The induced currents and electric fields for incident waves that propagate in forward direction are represented by arrows on the top

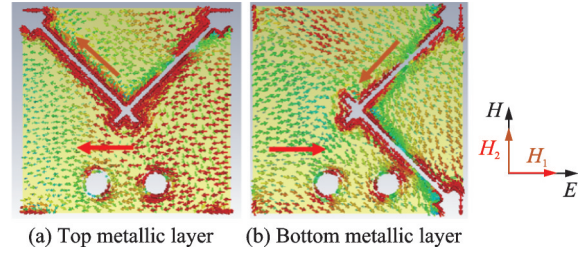


Fig.8 Surface current distribution on top and bottom metallic layers at resonance frequency 10 GHz of incident x -polarized wave

and bottom metallic layers in Figs.8(a, b), respectively. As illustrated in Fig.8, the induced electric and magnetic fields are initiated by the distribution of parallel and antiparallel currents on the top and bottom metallic layers. Therefore, it is possible to ascertain that the anti-parallel currents, which are sandwiched between the front and rear metallic layers, are unable to cancel the magnetic field, despite the fact that they generate a robust magnetic field in the substrate, in contrast to the parallel currents that are visible on the top and bottom layers of the structure. The induced magnetic fields in Fig.8 are represented by the letters H_1 and H_2 , as previously mentioned. These fields are generated by surface current distributions. As illustrated in Fig.8(a), the electric field component of the incoming wave is in alignment with H_1 , resulting in the transformation of the incident x -polarized EM wave to y -polarized as a result of polarization conversion during forward transmission. Therefore, in this instance, the x -polarized wave undergoes a transformation into an y -polarized transmitted wave during forward transmission.

Finally, Table 1 provides a comparative analysis of the proposed metasurface design and Refs.[15-17]. The comparison table suggests that the proposed multifunctional work demonstrates superior performance in a variety of parameters, including efficiency, angular stability, multifunctionality, and operating frequency bands. The metasurface with 0.787 mm thick was able to accomplish high transmission and PCR stable at up to 30° in Ref.[15]. The metasurfaces designed in Refs.[16-17] have an ultra-thin thickness, but they are not multifunctional, and the authors only claimed AT. Our proposed chiral metasurface accomplishes multifunctional op-

Table 1 Comparison between proposed work and previous published work

Ref.	Operating frequency band/ GHz	Transmission/%	PCR	Thickness/mm	Angular stability/(°)
Ref.[15]	8.58—9.73	90	90%	0.787	30
Ref.[16]	10—10.5	95	Not achieved	0.800	60
Ref.[17]	18.6—20.8	80	Not achieved	0.800	60
This work	8.3—10.4	95	95%	0.787	60

erations that are angularly stable to a maximum of 60° in the microwave regime, as a result of these studies.

3 Conclusions

A bi-layered, multifunctional chiral metasurface is reported in this paper. The suggested metasurface achieves AT and LPC in the frequency range from 8.3 GHz to 10.4 GHz with greater than 90% and 95% efficiency, respectively. The designed chiral metasurface also shows angular stability up to 60° for both operations of AT and LPC. This proposed chiral design can be used in applications based on the X-band frequencies.

References

- [1] WAN W, GAO J, YANG X. Metasurface holograms for holographic imaging[J]. *Advanced Optical Materials*, 2017, 5(21): 1700541.
- [2] LI S, CHEN Z N, LI T, et al. Characterization of metasurface lens antenna for sub-6 GHz dual-polarization full-dimension massive MIMO and multibeam systems[J]. *IEEE Transactions on Antennas and Propagation*, 2020, 68(3): 1366-1377.
- [3] SUN W, HE Q, SUN S, et al. High-efficiency surface plasmon meta-couplers: Concept and microwave-regime realizations[J]. *Light: Science & Applications*, 2016, 5(1): e16003.
- [4] HOSSAIN I, ISLAM M T, ALSAIF H, et al. An angular stable triple-band anisotropic cross-polarization conversion metasurface[J]. *Results in Physics*, 2022, 37: 105564.
- [5] LUO Y, QIU K, MOUMNI Z, et al. Chiral metasurface design with highly efficient and controllable asymmetric transmission and perfect polarization conversion of linearly polarized electromagnetic waves in the THz range[J]. *Journal of Physics D: Applied Physics*, 2022, 55(29): 295303.
- [6] JI W Y, CAI T, WANG G M, et al. High-efficiency and ultra-broadband asymmetric transmission metasurface based on topologically coding optimization method[J]. *Optics Express*, 2019, 27(3): 2844-2854.
- [7] AHMED A, CAO Q, KHAN M I, et al. A multifunctional broadband polarization rotator based on reflective anisotropic metasurface[J]. *Physics Letters A*, 2023, 470: 128785.
- [8] AHMED A, ABUTARBOUSH H F, AHMED F, et al. An efficient anisotropic metasurface for linear and circular-polarization conversion applications[C]// *Proceedings of 2020 14th European Conference on Antennas and Propagation (EuCAP)*. [S.l.] : IEEE, 2020: 1-3.
- [9] XU J, LI R, QIN J, et al. Ultra-broadband wide-angle linear polarization converter based on H-shaped metasurface[J]. *Optics Express*, 2018, 26(16): 20913-20919.
- [10] RASHID A, MURTAZA M, ZAIDI S A A, et al. A single-layer, wideband and angularly stable metasurface based polarization converter for linear-to-linear cross-polarization conversion[J]. *Plos One*, 2023, 18(1): e0280469.
- [11] XU H X, WANG G M, QI M Q, et al. Compact dual-band circular polarizer using twisted Hilbert-shaped chiral metamaterial[J]. *Optics Express*, 2013, 21(21): 24912-24921.
- [12] KHAN M I, TAHIR F A. A compact half and quarter-wave plate based on bi-layer anisotropic metasurface[J]. *Journal of Physics D: Applied Physics*, 2017, 50(43): 43LT04.
- [13] FEDOTOV V, MLADYONOV P, PROSVIRNIN S, et al. Asymmetric propagation of electromagnetic waves through a planar chiral structure[J]. *Physical Review Letters*, 2006, 97(16): 167401.
- [14] PLUM E, FEDOTOV V, ZHELUDEV N. Planar metamaterial with transmission and reflection that depend on the direction of incidence[J]. *Applied Physics Letters*, 2009. DOI:10.1063/1.3109780.
- [15] STEPHEN L, YOGESH N, SUBRAMANIAN V. Broadband asymmetric transmission of linearly polarized electromagnetic waves based on chiral metamaterial[J]. *Journal of Applied Physics*, 2018. DOI: 10.1063/1.5008614.
- [16] KHAN M I, HU B, AMANAT A, et al. Efficient asymmetric transmission for wide incidence angles using bi-layered chiral metasurface[J]. *Journal of Physics D: Applied Physics*, 2020, 53(30): 305004.
- [17] BIBI A, ISMAIL KHAN M, HU B, et al. Realizing efficient asymmetric transmission using optical activity

of ultrathin chiral metasurfaces for K-band applications[J]. *Microwave and Optical Technology Letters*, 2023, 65(8): 2443-2450.

Authors Mr. AFZAL Ahmed received the B.S. and M.S. degrees from COMSATS University Islamabad, Lahore Campus and Abbottabad Campus, Pakistan, in 2013 and 2017, respectively. He is currently pursuing the Ph.D. degree from Nanjing University of Aeronautics and Astronautics (NUAA), Nanjing, China. His research interests include antennas, metasurfaces and chiral metasurfaces.

Prof. CAO Qunsheng is a professor in the College of Electronic and Information Engineering at Nanjing University of Aeronautics and Astronautics (NUAA) in China. His cur-

rent research interests are in computational electromagnetics, meta-material, frequency-selective surface, antenna design, and signal integrity for high-speed circuits.

Author contributions Mr. AFZAL Ahmed designed the study, compiled the models and wrote the manuscript. Mr. MUHAMMAD Sajjad contributed to data analysis, result interpretation and manuscript revision. Prof. CAO Qunsheng contributed to the design, discussion and background of the study. All authors commented on the manuscript draft and approved the submission

Competing interests The authors declare no competing interests.

(Production Editor: ZHANG Huangqun)

具有不对称传输和线偏振转换的多功能手性超表面

AFZAL Ahmed, 曹群生, MUHAMMAD Sajjad

(南京航空航天大学电子信息工程学院, 南京 211106, 中国)

摘要:提出了一种多功能手性超表面来实现不对称传输(Asymmetric transmission, AT)和线偏振转换(Linear-polarization conversion, LPC)。设计的超表面由十字剑状形状和单元电池下侧的两个孔组成。在8.3~10.4 GHz频段,实现了90%以上的AT效率,并且相同的手性超表面将线偏振波高效地转换为正交波。对于LPC,偏振转换率(Polarization conversion ratio, PCR)大于95%。对于AT和LPC操作,所提出的超表面对于高达60°的电磁(Electromagnetic, EM)波入射角都是稳定的。

关键词:手性超表面;偏振转换;不对称传输;等离子共振